

## Seismic performance assessment of high-rise steel moment frame building with Reinforced Concrete (RC) core wall based on nonlinear time history analysis

Avaliação do desempenho sísmico dos arranha-céus momento da construção em aço com parede núcleo Betão Armado (BA) com base em análise não linear de histórico de tempo

Evaluación del desempeño sísmico de estructuras altas con sistema dual de marco de acero de flexión y núcleo de cortante Hormigón Armado (HA) basado en análisis no lineal de la historia del tiempo

Received: 02/27/2022 | Reviewed: 03/08/2022 | Accept: 03/12/2022 | Published: 03/20/2022

**Maryam Azodi**

ORCID: <https://orcid.org/0000-0002-1727-7191>  
Amirkabir University of Technology, Iran  
E-mail: Maryam.a94@aut.ac.ir

**Mehdi Banazadeh**

ORCID: <https://orcid.org/0000-0003-1562-3676>  
Amirkabir University of Technology, Iran  
E-mail: mbanazadeh@aut.ac.ir

**Amir Mahmoudi**

ORCID: <https://orcid.org/0000-0002-3098-9652>  
Amirkabir University of Technology, Iran  
E-mail: amirmahmoodiaut@gmail.com

### Abstract

This paper focuses on seismic responses of a 30-story high-rise building with a dual lateral system of Reinforced Concrete (RC) core shear wall and steel moment frame. To assess the seismic performance of the building, a nonlinear finite element model is built by using the OpenSees software. This three-dimensional model is created by using the fiber-beams for members and multi-layer shell elements for RC core walls. The numerical simulation has been examined under the thirteen sets of strong ground motion records which are scaled with the design and maximum seismic levels, Design-Basis Earthquake (DBE) and Maximum Considered Earthquake (MCE) level hazards respectively. In consequence, the desirable performance of high-rise steel moment frame building with RC shear core consisting of coupling beams and rectangular shear walls is shown. The outcome of nonlinear time history analyses reports the acceptable seismic performance of tall buildings designed. Results showed that maximum inter-story drift is significantly lower than allowable drift. Also, the RC core wall absorbed almost two-third of the total shear forces from the base level to one-third of height. However, the shear values of the core wall were significantly reduced by increasing the height while the shear values of the steel moment frame stayed constant.

**Keywords:** High-rise building; RC shear core; Nonlinear finite element model; Time history analysis; Seismic performance.

### Resumo

Este artigo enfoca as respostas sísmicas de um edifício de 30 andares com um sistema de parede de cisalhamento lateral duplo Betão Armado (BA) e estrutura de aço resistente ao momento. Para avaliar o comportamento sísmico do edifício, um modelo de elementos finitos não linear é construído usando o software OpenSees. Este modelo tridimensional é criado usando vigas de fibra para membros e elementos de revestimento multicamadas para paredes de núcleo BA. A simulação numérica foi examinada sob os treze conjuntos de registros de movimento do solo fortes que são dimensionados com os níveis sísmicos máximo e de projeto, Acidente de Base de Projeto (ABP) e Risco Sísmico Máximo (RSM), respectivamente. Conseqüentemente, o desempenho desejável da construção de estrutura de aço de arranha-céus com núcleo de cisalhamento BA consiste em vigas de acoplamento e paredes de cisalhamento retangulares. O resultado das análises de histórico de tempo não linear informa o desempenho sísmico aceitável de edifícios altos projetados. Os resultados mostraram que a razão de deriva máxima entre pisos é significativamente menor que a deriva permitida. Além disso, a parede do núcleo BA absorveu quase dois terços das forças de cisalhamento totais desde o nível da base até um terço da altura. No entanto, os valores de cisalhamento da parede do

núcleo diminuíram significativamente com o aumento da altura, enquanto os valores de cisalhamento do pórtico de aço permaneceram constantes.

**Palavras-chave:** Arranha-céus; Núcleo de cisalhamento BA; Modelo de elementos finitos não lineares; Análise de histórico de tempo; Vulnerabilidade sísmica.

### Resumen

Este artículo se enfoca en las respuestas sísmicas de un edificio de gran altura de 30 pisos con un sistema dual de marco de acero a flexión y núcleos de corte (RC) de hormigón armado. Para evaluar el desempeño sísmico del edificio, se construyó un modelo de elementos finitos no lineal utilizando el software OpenSees. Este modelo 3D se creó utilizando fiber-beam para miembros y elementos de multi-layer shell para paredes de núcleo de RC. Las simulaciones numéricas se examinan bajo trece conjuntos de registros del movimiento fuerte de la tierra que se escalan con los niveles de diseño y sísmico máximo, terremoto basado en el diseño (DBE) y sísmico máximo (MCE), respectivamente. Como resultado, se muestra el rendimiento óptimo de la estructura de marco de flexión de acero de gran altura con núcleo de corte RC que consta de vigas de acoplamiento y paredes de corte rectangulares. Los resultados de los análisis de la historia del tiempo no lineales informan el desempeño sísmico aceptable de los edificios altos diseñados. Los resultados mostraron que la deriva máxima entre pisos es significativamente menor que la deriva permitida. Además, la pared del núcleo de RC absorbe aproximadamente dos tercios del total de las fuerzas de corte desde la superficie de la base hasta un tercio de la altura. Sin embargo, los valores de cortante de la pared del núcleo disminuyeron significativamente con el aumento de la altura, mientras que los valores de cortante del marco de acero a flexión permanecieron constantes.

**Palabras clave:** Estructura alta; Sistema dual de marco de flexión de acero; Núcleo de corte RC; Análisis de historial de tiempo no lineal; Desempeño sísmico.

## 1. Introduction

Nowadays, the construction of high-rise structures has been demanded even in seismic hazardous zones. Thus, serious researches have been conducted to investigate their performance. For the medium to high-rise buildings in seismic hazardous zones, Reinforced Concrete (RC) core walls have been developed as the key element for resisting seismic lateral loads. The RC shear walls or shear cores consist of several rectangular sections which are usually placed in the elevator or stair shafts due to their shapes. The main function of RC structural walls is to resist lateral loads. According to Azam and Hosure (2013), including the shear walls in tall buildings provides a significant improvement on their lateral strength. Also placement of shear walls symmetrically in the outermost moment-resisting frames and preferably interconnected in a mutually perpendicular direction forming the core will provide better seismic performance in terms of strength and stiffness (Azam & Hosur, 2013). Due to higher stiffness of steel RC shear walls in comparison with other types of RC walls such as Super Elastic Shape Memory Alloy bars (SE-SMA) in RC shear walls, the lateral displacement of steel RC walls is less than SMA shear walls up to 10%. However, the residual displacements of RC shear walls are more than SMA RC walls for moderate to extreme ground motion records by 19-50% (Abraik et al., 2020). Abraik and Youssef (2018) presented that the well performance of steel and SMA RC walls under seismic events and it was negligible difference exists between steel and SE-SMA walls in term of inter-story drifts.

Although RC core wall systems have been widely used in recent years supported by extensive studies to explore their behavior under various loading conditions, their actual seismic behavior is poorly understood. Many early researches indicated that numerical simulation is advantageous for nonlinear seismic analysis of such structures. Lu et al. (2015) and have studied the modeling of integrating fiber-beam elements and shell multilayer elements for super-tall buildings in OpenSees (McKenna, 2011). In another study, Lu et al. (2018) have compared the seismic design of the tall RC frame core tube structure in China and USA seismic design code by using MSC Marc program. Arabzadeh and Galal (2017) also modeled the shell element for the simulation of non-planer C-shaped RC shear walls. Whereas several researches have been conducted by various finite element software, the OpenSees contains a fair capability for simulating the RC shear core. Three dimensional simulation in OpenSees can include to cyclic degradation of the material behavior, effect of transverse tensile strains on the compressive

strength of concrete in walls, wall coupling effects, and compensation for mesh-size effects (Zhang et al., 2017).

Many studies have shown that the lateral response of high-rise structures with core walls is dominated by the special behavior of the coupling beams. The RC walls are designed to increase the lateral resistance of such structures. They provide significant strength, stiffness, and deformation capacity or energy dissipation capacity of the high-rise structures to meet seismic demands (Azam & Hosur, 2013). Arabzadeh and Galal (2018) researched on nonlinear time history analysis of C-shaped RC walls which design as a RC core wall for 16-story RC building. According to their results, significant contribution of higher modes noticeably affects story shear forces. The lateral response of taller buildings is mainly controlled by flexural deformations. Under earthquake-induced lateral loading, the coupling beams yield first and suffer from considerable plastic deformation. In addition to their own flexural capacities, adjacent wall piers are subjected to the axial forces transferred from coupling beams and thus can form a tension-compression force couple to resist the earthquake-induced moment (Wu et al., 2019). So they provide more lateral stiffness and less bending moment in each wall. To evaluate the progressive collapse resistance of the RC shear wall, Ren et al. (2015) have created a finite element models simulating of two typical 15-story RC frame shear wall structures. Their results revealed that the shear walls in the form of “C” or tube-shape provide functional requirements because they provide the adequate alternative load path in the interconnected shear walls. In the other researchers' studies, more energy dissipation have been reported compared to the single walls, due to the inelastic deformations of coupling beams (Harries, 2001), (Constantin, 2016). The coupled RC walls have considerable ability to control the inter-story drift; so this structural system is highly efficient in reducing the damage of non-structural elements (Constantin, 2016). The coupling action which transfers vertical forces between adjacent walls has three major beneficial effects; reducing the moments in the individual walls, undergoing inelastic deformations to provide a mean by which seismic energy is dissipated over the entire height of the wall system, and its lateral stiffness is significantly greater than the sum of its component wall piers, permitting a reduced footprint for the lateral load resisting system (El-Tawil et al., 2009).

There has been a limited number of previous to standardized the seismic performance of the steel moment frame with RC core. So the current research develops an effective three-dimensional numerical model of a 30-story, high-rise structure, with a dual lateral load-resistant system of the Intermediate Moment-resisting Steel Frame (IMSF) and RC shear core using OpenSees software to evaluating the nonlinear seismic behavior of the model based on the relevant guidelines and regulations at Design-Basis Earthquake level (DBE) and Maximum Considered Earthquake level (MCE).

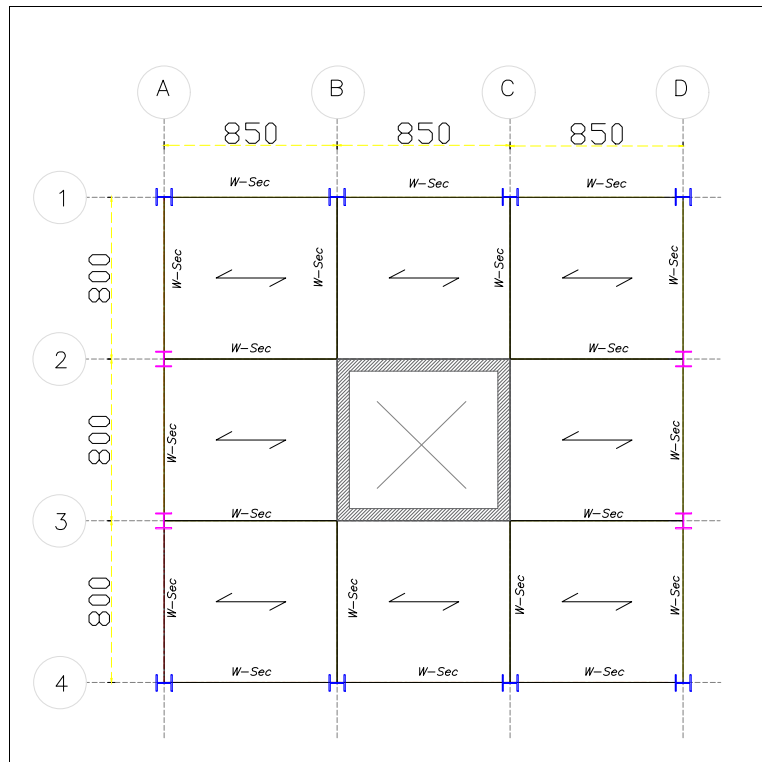
## **2. Methodology**

### **2.1 Input Model Assumptions**

#### **2.1.1 Building Description**

The present study is performed a three-dimensional model in ETABS (2016) and OpenSees software. The numerical example has a plan dimensions of  $24\text{ m} \times 25.5\text{ m}$  with a bay length of  $8.5\text{ m}$  in the X-direction and  $8\text{ m}$  in the Y-direction with total height  $108.6\text{ m}$ ,  $4.2\text{ m}$  for base floor height and  $3.6\text{ m}$  for the other twenty-nine stories. Furthermore, as shown in Figure 1, an  $8.5 \times 8\text{ m}$  opening in the middle part of the plan is considered to locate the staircase and elevator where the shear walls are modeled as the shear core with two C-shaped walls connected by coupling beams. It was assumed that the 30-story building is located at California region with a longitude of  $-121.15$  and a latitude of  $37.51$ . Moreover, the site has classified in type C soil with the shear velocity ranging from  $370\text{ m/s}$  to  $762\text{ m/s}$ .

**Figure 1:** The plan of the studied building (dimensions in mm).



Source: Authors.

Firstly, to design the wall sections, column and beam members, a three-dimensional model is simulated on ETABS (2016) software. Material properties details are illustrated in Table 1. Table 2 shows the details of loading on members and one-way slabs according to ASCE7-16 (2016). All of the column and beam sections are adopted W-section (Figure 1). RC core walls are also modeled by rectangular sections with uniform rebar distribution. The analytical fundamental periods of the building are calculated as 2.861 s and 2.517 s in principal directions, for the first and second modes, in ETABS software. Table 3 represents the details of designing reinforcement of shear walls and coupled beams. The allowable percentage of longitudinal and transverse reinforcement ( $\rho$ ) for shear walls have to be between 0.25% and 4%., respectively. Moreover, the percentage of longitudinal reinforcement for coupling beams are limited between 0.4% and 2.5%.

**Table 1:** Material properties.

|            | Numerical Strength<br>(Kgf/ mm <sup>2</sup> ) | Expected Strength<br>(Kgf/ mm <sup>2</sup> ) | Modulus of<br>Elasticity(Kgf/<br>mm <sup>2</sup> ) | Specify Weight<br>(Kgf/m <sup>3</sup> ) | Poisson's<br>Ratio |
|------------|---|--|--|---|--------------------|
| Steel ST52 | 35.15   | 38.86  | 20390  | 7850                                    | 0.3                |
| Concrete   | 4   | 5.2  | 3023   | 2500                                    | 0.2                |
| Rebar Gr60 | -   | 61.18  | 20390  | 7850                                    | -                  |

Source: ACI Committee 318, 2014.

**Table 2:** Loading details.

| Earthquake Load  |                       | Gravity Loads        |             | Snow Load    |
|--|-----------------------|----------------------|-------------|--------------|
| R Response Modification Factor                             | 6                     | Dead Load (stories)  | 450 Kgf/ m2 | 24.4 Kgf/ m2 |
| $\Omega$ Safety factor                                     | 2.5                   | Dead Load (Roof)     | 550 Kgf/ m2 |              |
| Cd Deflection Amplification                                | 5                     | Dead Load (Walls)    | 500 Kgf/ m  |              |
| Factor   | 0.02                  | Live Loads (stories) | 200 Kgf/ m2 |              |
| Ct building period coefficient x level under consideration | (USA),<br>0.0488 (SI) | Live Load (Roof)     | 290 Kgf/ m2 |              |
| h; height of building                                      | 108.6 m               |                      |             |              |
| $T_a = C_t * h^x$ Approximate Fundamental Period           | 0.75<br>1.64 sec      |                      |             |              |

Source: ASCE7-16 (2016)

**Table 3:** Designing reinforcements for shear walls and coupled beams.

| Wall thickness (cm) | Percentage of longitude rebar $\rho$ | Transvers rebar per meter (mm2/m) | Beam thickness (cm) | Longitude rebar per meter (mm2/m) | Transverse rebar (mm2) |
|---------------------|--------------------------------------|-----------------------------------|---------------------|-----------------------------------|------------------------|
| 60                  | 0.0046                               | 1600                              | 60                  | 4800                              | 6400                   |
| 55                  | 0.0053                               | 1375                              | 55                  | 4000                              | 5400                   |
| 50                  | 0.0058                               | 1250                              | 50                  | 2500                              | 3300                   |
| 40                  | 0.0068                               | 1000                              | 40                  | 2200                              | 3000                   |
| 30                  | 0.0086                               | 750                               | 30                  | 2000                              | 2700                   |

Source: Authors.

### 2.1.2 Ground Motion Selection

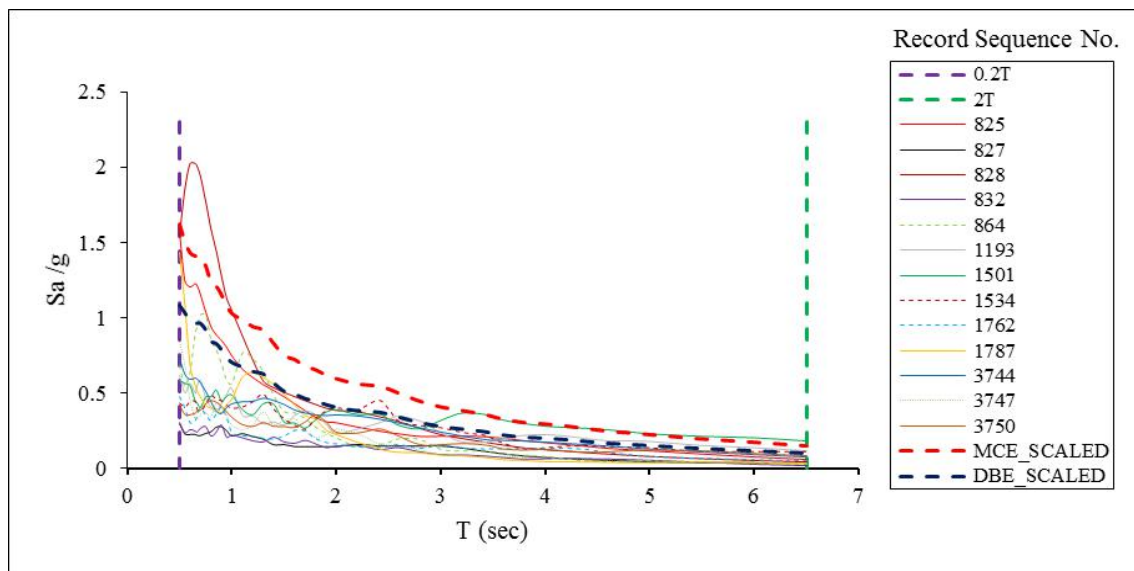
In order to evaluate the seismic performance of the high-rise structure, thirteen strong ground motions set are selected in the current study as described by FEMA P695 (Huret, 2017). For nonlinear time history analysis, two horizontal components available for each record are treated as independent motions following the FEMA P695 (ATC, 2009). These selected records are scaled with the design and maximum seismic levels (DBE and MCE). These intense seismic records were selected from the Pacific Earthquake Engineering Research center (PEER) database (Mosalam et al., 2011) with a magnitude greater than 7 Richter. The maximum response spectrum and mean response spectrum are determined for each pair of accelerograms. According to ASCE7-16, the value of this spectrum falls within the allowable period range (between  $0.2T$  and  $2T$ ) and should not be less than 90% of the corresponding value in the target response spectrum (ASCE7-16, 2016). The considered records need to be selected with frequencies below 0.1Hz because the long-term excitation is obtained for evaluating the structural performance (Moehle et al., 2011). The specifications of the selected records are illustrated in Table 4. Besides, Figure 2 shows the maximum response spectrum functions with RSN (Record Sequence Number) which are scaled with designed and maximum seismic level hazards.

**Table 4:** Specification of selected ground motion records.

| Record | Record Sequence Number (RSN) | Earthquake Name | Year | Station Name            | Magnitude | Frequency (Hz) |
|--------|------------------------------|-----------------|------|-------------------------|-----------|----------------|
| 1      | 825                          | Cape Mendocino  | 1992 | Cape Mendocino          | 7.01      | 0.07           |
| 2      | 827                          | Cape Mendocino  | 1992 | Fortuna - Fortuna Blvd  | 7.01      | 0.07           |
| 3      | 828                          | Cape Mendocino  | 1992 | Petrolia                | 7.01      | 0.07           |
| 4      | 832                          | Landers         | 1992 | Amboy                   | 7.28      | 0.1            |
| 5      | 864                          | Landers         | 1992 | Joshua Tree             | 7.28      | 0.07           |
| 6      | 1193                         | Chi-Chi_Taiwan  | 1999 | CHY024                  | 7.62      | 0.025          |
| 7      | 1501                         | Chi-Chi_Taiwan  | 1999 | TCU063                  | 7.62      | 0.0375         |
| 8      | 1534                         | Chi-Chi_Taiwan  | 1999 | TCU107                  | 7.62      | 0.0375         |
| 9      | 1762                         | Hector Mine     | 1999 | Amboy                   | 7.13      | 0.08           |
| 10     | 1787                         | Hector Mine     | 1999 | Hector                  | 7.13      | 0.0375         |
| 11     | 3744                         | Cape Mendocino  | 1992 | Bunker Hill FAA         | 7.01      | 0              |
| 12     | 3747                         | Cape Mendocino  | 1992 | College of the Redwoods | 7.01      | 0.0625         |
| 13     | 3750                         | Cape Mendocino  | 1992 | Loleta Fire Station     | 7.01      | 0.0625         |

Source: Authors.

**Figure 2:** Ground motion response spectra of selected ground motions for 5% damping.



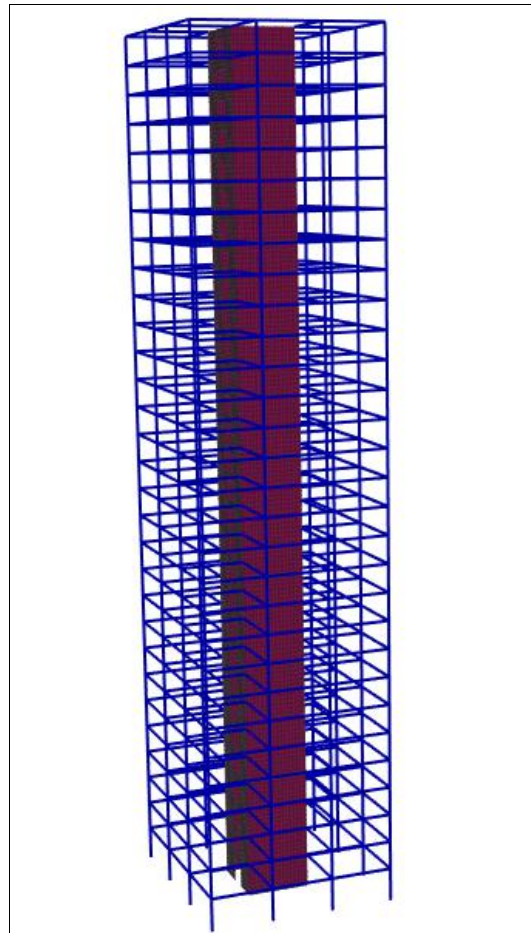
Source: Authors.

## 2.2 Numerical Model Description

As conventional structural analysis programs, such as ETABS, do not allow nonlinear modeling of some elements, it is necessary to take an alternative approach to assess the nonlinear response of the shear wall elements. OpenSees software has mainly been applied to analyze the responses of structures under seismic loadings. Besides, it can carry out the static linear, pushover, modal, dynamic nonlinear analysis, etc. Furthermore, it is an open-source system and allows the researchers to add new materials constitutions and new types of elements, such as multi-layer shell elements for simulating RC core walls (Lu et al., 2018). In this study, an inelastic three-dimensional 30-story building with a dual lateral system consisting of RC core wall and steel moment frame is simulated using OpenSees. The frame beams and columns are simulated with fiber beam elements, and multi-layer shell elements are used to model the core tube and the coupling beams which exhibit superior nonlinear performance. Besides, truss elements are adopted to simulate the longitudinal and diagonal reinforcements in boundary

elements and coupling beams (Constantin, 2016). Therefore, the beams and columns sections are simulated with fiber sections due to the accurate calculation can be achieved. Beams with hinges at the end sides are simulated by ElasticBeamColumn elements (Figure 1) and all of the columns members and other beams members are modeled as dispBeamColumn elements. Although the slabs are not modeled in OpenSees, nodes of each floor are assigned as a rigid diaphragm. According to Lu et al. (2015), the multi-layer shell elements are used to simulate the high-rise core wall and coupled beams based on shell MITC4 element in OpenSees. The multi-layer shell element is based on principal of composite material mechanism and can be simulated in coupled in-plane / out-plane bending, and also in-plane bending-shear nonlinear behavior of structural shell element. This special flat shell element consisting of planner membrane element and plate bending element. The two-dimensional concrete material and the reinforced steel material are introduced for multi-layer shell elements, and the section is divided by each material and its thickness. Figure 3 illustrates the project model with core wall.

**Figure 3:** 3D modeled structure with the core shear wall.



Source: Authors.

### 2.3 Nonlinear Analysis

In this study, a modal analysis is carried out for both ETABS and OpenSees models. The first and second periods of the structure have obtained by conducting a modal analysis in OpenSees, and they are 3.168 sec and 2.53 sec, respectively.

Also as a modal analysis of case study in ETABS, the first and second periods calculated 2.86 sec and 2.517 sec, respectively. Due to differences in simulating materials of the case study in ETABS and OpenSees, the result of modal analysis and the total gravity weight of models revealed a little difference. According to the comparison between calculated periods from ETABS and OpenSees software, the differences between the first modes and second modes obtained from the two programs are 10% and 0.07%, respectively. Furthermore, the structure gravity weight in ETABS is almost 14326 tonf and in OpenSees is 14451 tonf, which shows an about 1% difference. Because of the considerable contribution of the first three modes, it is reasonable to use the inverted triangular distribution of lateral loads. For nonlinear static pushover analysis, it is necessary to determine the target displacement (ASCE/SEI 41-17, 2017), which is shown as Eq. 1:

$$\delta_t = C_0 C_1 C_2 S_a \times \frac{T_e^2}{4\pi^2} \times g \quad (1)$$

Where  $S_a$  or  $PGA$  is the Response spectrum acceleration at the effective fundamental period and damping ratio of the building in the direction of interest it was 1.65 for MCE and 1.1 for DBE level hazards using the USGA site.  $C_0$  is the Modification factor to relate spectral displacement of an equivalent single-degree-of-freedom (SDOF) system to the roof displacement of the building multi-degree-of-freedom (MDOF) system calculated 1.3 according to ASCE/SEI 41-17 (2017). Also,  $T_e$  is the Effective fundamental period of the building in the direction under consideration. The  $C_1$  is the modification factor to relate expected maximum inelastic displacements to displacements calculated for linear elastic response and  $C_2$  is the modification factor to represent the effect of pinched hysteresis shape, cyclic stiffness degradation, and strength deterioration on the maximum displacement response. In conclusion,  $C_1$  and  $C_2$  factors are 1 and 0.7, respectively, when the period of the structure is greater than 1 sec. From the Eq. 1, the target displacements for the MCER level are 3.9 m and 2.6 m in X and Y-directions, respectively, and they are 2.6 m in the X-direction and 1.75 m in the Y-direction for the DBE level. Based on the previous studies on nonlinear analysis results of high-rise structures, 6% is found to be an appropriate mean value for the collapse limit (Esteghamati et al., 2018). So in this study, the target displacement is assumed as 6.5 m (6% of the structure height) in both directions. A set of thirteen pairs of intense ground motion records being listed in Table 4 with magnitudes greater than 7 Richter and frequencies lower than 0.1 Hz are selected from the PEER database for time history analysis. These records are generated for reference soil type C and scaled with DBE and MCE level hazards (Figure 2).

### 3. Analysis Results and Discussions

The time history analysis and pushover analysis are performed on the structure introduced in section 3. This numerical model is created in OpenSees software based on ASCE/SEI 41-17 and Lu et al. (2015). Its sections of the members obtained from ETABS (2016) design. The maximum displacements of the structure are resulted from ETABS software, reported in Table 5 in two directions under the DBE level hazard. It is observed that all of the displacements are much lower than allowable displacement.

**Table 5:** Roof displacement in two directions calculated by ETABS (2016).

| Story | Dir. | Displacement (mm) | Disp.*Cd (mm) | Allowable Disp. (mm) |
|-------|------|-------------------|---------------|----------------------|
| 30    | X    | 10.767            | 59.2185       | 72                   |
| 30    | Y    | 11.867            | 65.2685       | 72                   |

Source: Authors.



### 3.1 Pushover Analysis

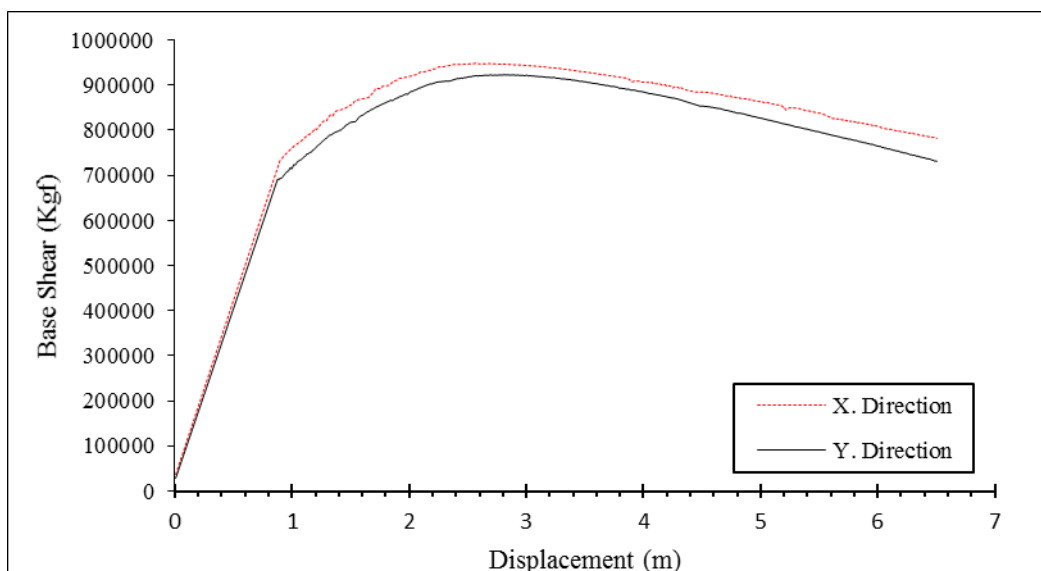
According to Saleemuddin et al. (2017), The pushover analysis is promising simple and efficient approach of evaluation of inelastic lateral loads resistance of large class of structures, provided that its limitations are fully addressed. Previous results showed that inelastic deformation increases with increase in story height of structures in RC structures (Saleemuddin et al., 2017). So the pushover analysis has been suitable option to predict elastic and inelastic behavior of high-rise structures. In this study, the nonlinear static analysis or pushover analysis is performed using OpenSees software. The results of pushover analysis are extracted and illustrated in Figure 4. It can be seen that the maximum base shear for both directions is strikingly equal. Since the pushover analysis was performed before earthquake applied the inelastic behavior of case study cannot be predicted. The elastic performance of the high-rise building was showed which was acceptable.

Even though the plan of the high-rise building is symmetrical, due to one-way slab which applied gravity loads on horizontal beams, it is observed the base shear values are a little different in X and Y directions. Furthermore, the placement of columns effected on this discrepancy between shear vales and pushover curves. According to ASCE/SEI 41-17 (2017), the ratio of elastic strength demand to yield strength coefficient calculated in accordance with Eq. 2:

$$\mu_{strength} = \frac{S_a}{V_y/W} * C_m \quad (2)$$

Where  $V_y$  is the yield strength of the structure in the direction of interest,  $W$  is the effective seismic weight, and  $C_m$  is the effective mass factor (ASCE/SEI 41-17, 2017).

**Figure 4:** Pushover analysis curves for X and Y directions.



Source: Authors.

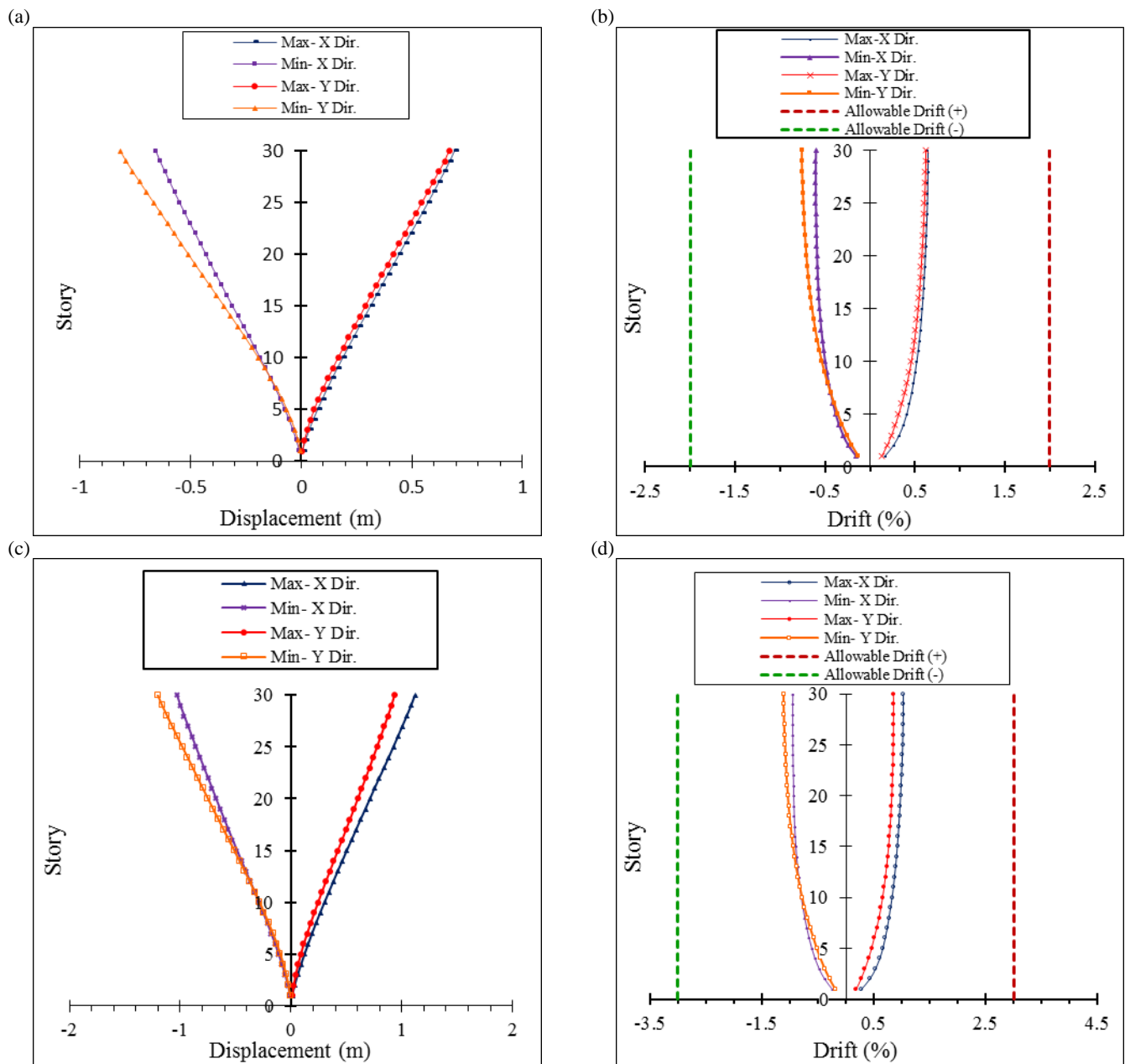
The strength ratios of the building are calculated at 3.068 and 3.275 in X and Y directions, respectively, which are significantly lower than the maximum strength ratio introduced in ASCE41 code (the maximum strength ratios are 10.37 and 8.467 in X and Y directions). As a result, buildings with RC core walls modeled using multi-layer shell elements are validated as a great resistance system.

### 3.2 Time history analysis

To evaluate the behavior of the high-rise structures under the strong ground motion records, the code of FEMA P695 (ATC, 2009) had demanded the nonlinear time history analysis. The time history analysis of the structure has performed in both earthquake levels (DBE and MCE) and the maximum inter-story drifts, maximum inter-story displacements, maximum floor accelerations, and maximum shear forces of both core wall and moment frame along the height are extracted from the results of the analysis of the model created in ETABS. In the DBE level earthquake hazard, for instance, the maximum displacements of the roof center of mass have been calculated by applying the strongest seismic record, Chi-Chi earthquake with a magnitude of 7.62 Richter and the Cape Mendocino earthquake (second strongest seismic record) with the magnitude of 7.01 Richter (Table 4). They are 0.9 and 1.7 m in the X and Y directions, respectively. Also, the maximum average displacement in the X and Y directions are 71 and 88 cm on the roof center of mass, respectively. The displacement results of the DBE level are illustrated in Figure 5-a. The maximum average story drift in both X and Y directions was 0.81% on the 29<sup>th</sup> floor at the design seismic level hazard (Figure 5-b), which is far below the allowable drift at this level (2%) (ASCE, 2014).

The maximum displacement of the roof center of mass in the X and Y directions is 1.8 and 2.5 m, respectively, in MCE level hazard. Also, the average maximum roof displacement in the X is 1.1 m and in the Y directions is 1.25 m at the MCE seismic level. The average maximum story drift occurred on the 29<sup>th</sup> floor equal to 1.03% in X direction and 1.10% in the Y directions. Despite the applied strong accelerograms, the happened drift values in both directions are far lower than the allowable value (3%), which indicates the significant stiffness of the shear core under the lateral load. Figure 5-c and Figure 5-d indicates the inter-story displacement and drift in MCE level, respectively.

**Figure 5:** (a) The average of maximum stories displacements in DBE level (b) The average of maximum stories drifts in DBE level (c) the average of maximum stories displacements in MCE level (d) the average of maximum stories drifts in MCE level.

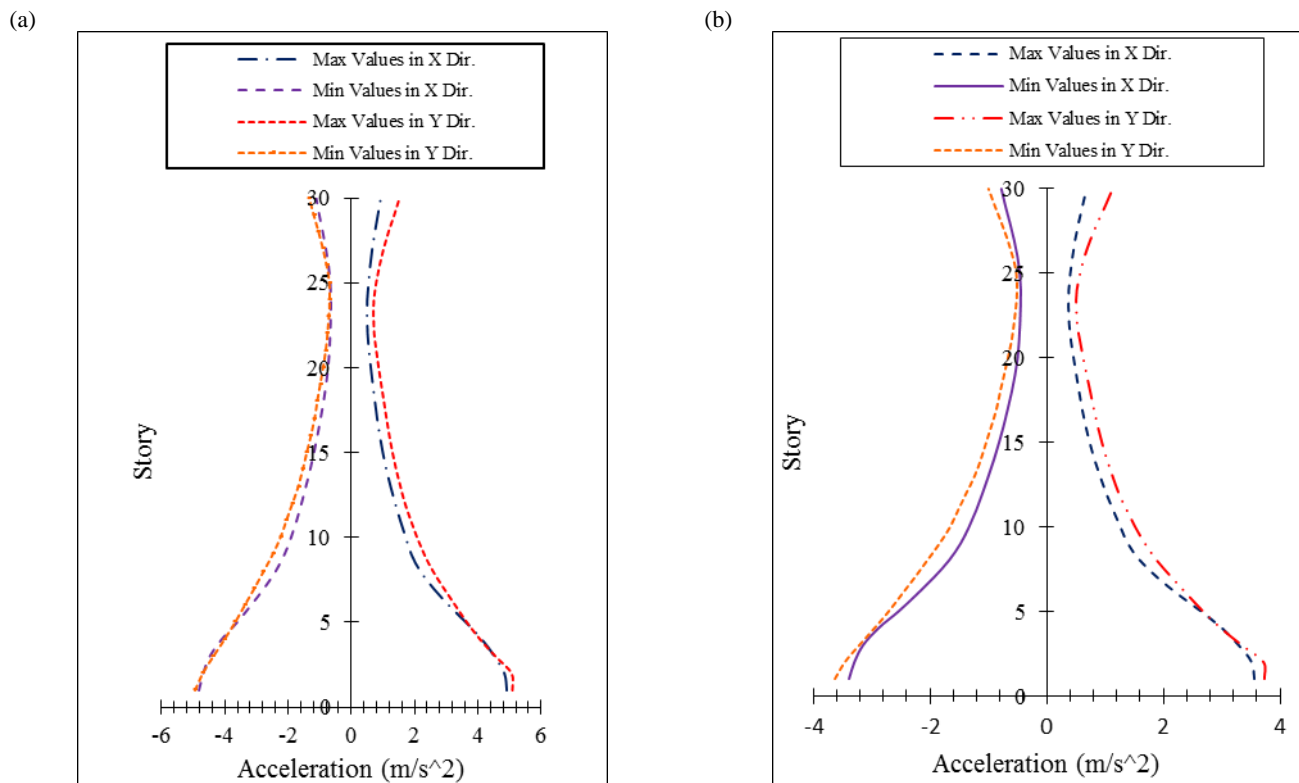


Source: Authors.

The floor acceleration distribution is schematically identical for all records, although they are very different in value because they have very different PGA values. The highest acceleration in the DBE level belongs to one of the records with the PGA value of  $36.33 \frac{m}{s^2}$ , which is  $9.87 \frac{m}{s^2}$  and  $10.02 \frac{m}{s^2}$  in the X and Y directions, respectively. In design level, the average maximum acceleration occurred on the first floor, which was  $3.67 \frac{m}{s^2}$  and  $3.87 \frac{m}{s^2}$  in the X and Y directions, respectively, and the lowest acceleration on the 24<sup>th</sup> floor was  $0.43 \frac{m}{s^2}$  and  $0.49 \frac{m}{s^2}$  in the X and Y directions, respectively. The Figure 6-a

illuminates the distribution of the average of maximum story acceleration DBE. As for the DBE seismic level, the maximum acceleration belongs to one of the records in the X and Y directions equal to  $13.59 \frac{m}{s^2}$  and  $13.36 \frac{m}{s^2}$ , respectively. Also, the average maximum acceleration occurred on the first floor, which was  $4.93 \frac{m}{s^2}$  and  $5.09 \frac{m}{s^2}$  in the X and Y directions, respectively, and the average minimum acceleration on the 24<sup>th</sup> floor was  $0.51 \frac{m}{s^2}$  and  $0.69 \frac{m}{s^2}$  in the X and Y directions, respectively. According to Figure 6-a and Figure 6-b, the second floor has the highest acceleration along with the structure height. Then, the maximum acceleration of stories is decreased from this level up to the 24<sup>th</sup> floor (nearly up to 3/4 of the structure height), and eventually, it is increased to the roof. The average of maximum floor accelerations is illustrated in Figure 6-a and Figure 6-b for DBE and MCE level hazards, respectively.

**Figure 6:** (a) Distribution of Average of maximum stories acceleration in DBE level (b) Distribution of Average of maximum stories acceleration in MCE level.

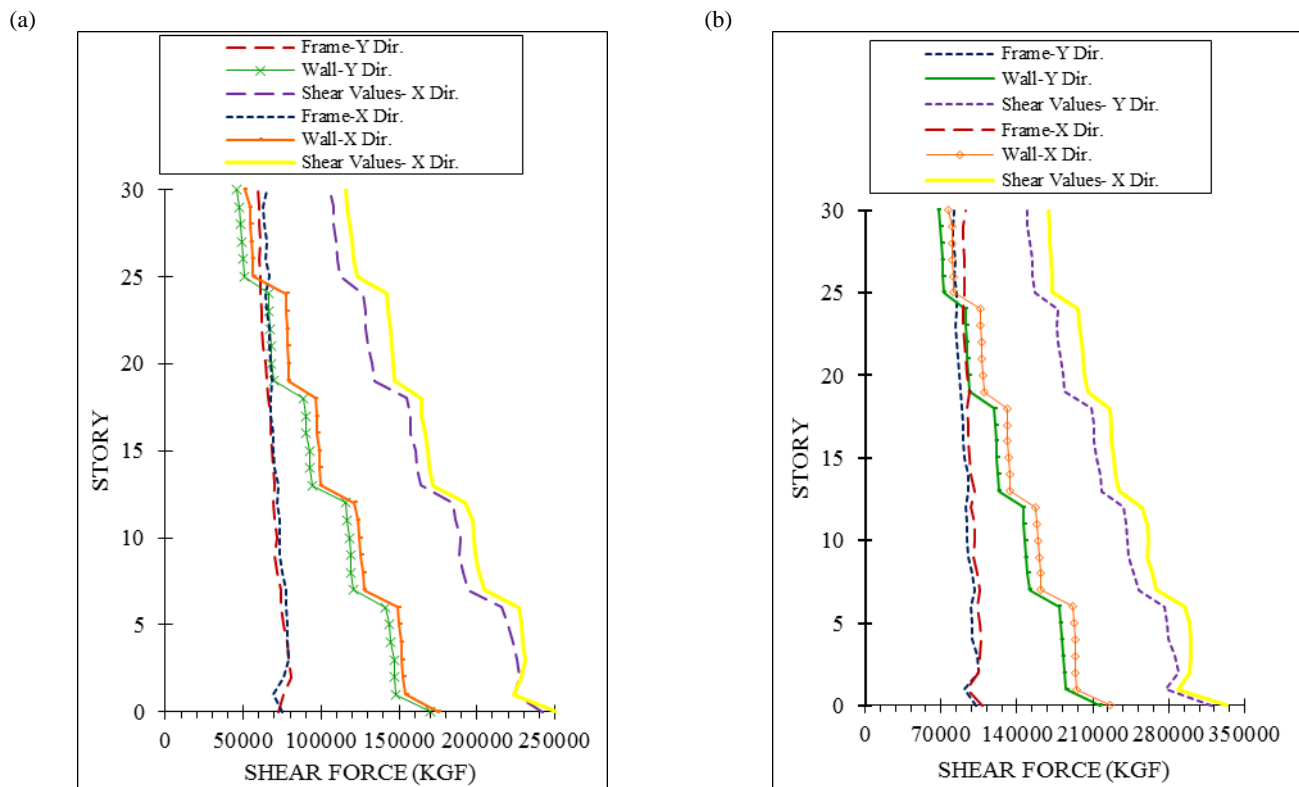


Source: Authors.

Figure 7 compares the vertical distribution of story shear at the instants of maximum base shear, for frame and core wall under design and maximum hazard levels. The vertical distribution of story shears is similar for both level hazards; however, the peak value of base shear in DBE is almost 240000 kgf, and in MCE level, it is about 300000 kgf. Although the distribution of story shear over the structure height is alike for both directions, the maximum story shear in X direction is a little higher than Y direction for both hazard levels. Under the DBE and MCE level, the maximum core wall shear forces are almost 180000 kgf and 220000 kgf, respectively, which are approximately twice than maximum frame shear forces. The shear forces resisted by the core shear wall and the ordinary moment frame (OMF) are essentially constant over the building height;

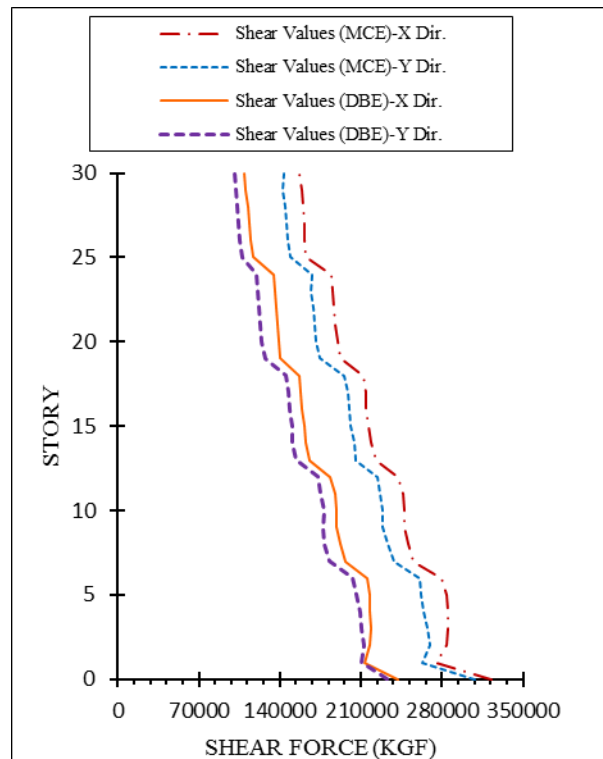
however, the peak values of core wall shear forces are significantly affected by shear wall thicknesses. Under both level hazards, the OMF resisted about one-third of story shear at the base level to 10th floor, then core shear forces gradually decreased; therefore, the thicker shear wall can resist more story shear. According to observation, the shear values of OMF are approximately equal to core wall shear forces from the 20th floor to the roof level. It is observed that the distribution of the story shear in the OMF did not follow a particular trend, and it was almost uniform throughout the structure height. It is also reduced at the second level for most records. Moreover, the distribution of shear forces in the structure height is shown in Figure 8 for DBE and MCE level hazards. It is observed stories shear values in X direction is slightly more than Y direction due to the applied gravity loads and placement of columns.

**Figure 7:** The distribution of the average of total shear values in the structure height in (a) DBE level (b) MCE level.



Source: Authors.

**Figure 8:** Comparison of the mean total shear force in the X and Y directions for DBE and MCE level hazards.



Source: Authors.

#### 4. Conclusion

A nonlinear time history analysis of a three-dimensional 30-story building with a dual lateral system consisting of RC core shear wall and steel moment frame is carried out with OpenSees, a finite element program based on fiber-elements. Prior studies developed new code as a multi-layer shell element using OpenSees for modeling shear walls and shear core walls in a high-rise building, which is used in the current study for the three-dimensional simulation of RC core wall in the 30-story building. In order to assess the seismic performance of a super-tall building with dual lateral resisted system, time history analysis using thirteen sets strong ground motion records are performed, and results showed the following:

- Because the stiffness of the structure is approximately equal in both X and Y directions, the distribution of maximum displacement, drift, acceleration, and shear values along the structure height for the design and maximum seismic levels is identical in the two directions.
- According to the distribution of maximum story drift in both X and Y directions and both seismic levels, the slope of drift curve from the first to the middle floors of the building is large and decreased from the middle floors, continuing as the straight line to the roof. The highest drift is also created for both directions and seismic levels at the 29<sup>th</sup> level.
- Due to the distribution of maximum acceleration at the structure height, the highest acceleration occurred on the first floor and the lowest one on the 24<sup>th</sup> floor, as the acceleration was decreased about 80% from its maximum value to the 24<sup>th</sup> floor (for both directions and seismic levels) and then, increased to 50% from that level to the roof.
- The maximum shear value of the wall from the base level to about 1/3 of the structure height is twice that of the maximum shear in the frame. Since the shear values of the wall are dependent on the thickness of walls and

significantly reduced in height but the maximum shear values of the frame that do not follow a specific trend, are almost uniform throughout the structure height. Thus, in the upper floors, the shear value of the wall is equal, and even in the upper six floors of the structure, this value is less than the frame shear.

- Given the distribution of maximum shear of the frame, wall and whole floor over the structure height, the share of the wall shear from the base level to about 1/3 of the structure height is equal to 2/3 of the total story shear, and the higher the height, the lower the shear resisted by the wall, so that in the upper six floors, it is less than half the total shear. It was shown, the maximum story shear value from the base level to the roof is reduced by about 50-60% with a specific trend for all accelerograms applied in both directions and both seismic hazard levels.

It is possible to extend the approach to the assessment of the seismic response of other types of high-rise buildings with dual lateral systems for future research. For example, seismic performance of two types of buildings consisting of moment frame and RC core walls that one of their systems is steel moment frame and another one is RC moment frame could be compared. Also, modeling and seismic performance assessment of high-rise moment frame structure with RC core walls and steel connecting beams are suggested.

## References

- Abraik, E., El-Fitiany, S. F., & Youssef, M. A. (2020). Seismic performance of concrete core walls reinforced with shape memory alloy bars. *Structures*, 27(April), 1479–1489. <https://doi.org/10.1016/j.istruc.2020.07.053>
- Abraik, E., & Youssef, M. A. (2018). Seismic fragility assessment of superelastic shape memory alloy reinforced concrete shear walls. *Journal of Building Engineering*, 19(May), 142–153. <https://doi.org/10.1016/j.job.2018.05.009>
- Arabzadeh, H., & Galal, K. (2017). Seismic Collapse Risk Assessment and FRP Retrofitting of RC Coupled C-Shaped Core Walls Using the FEMA P695 Methodology. *Journal of Structural Engineering*, 143(9), 04017096. [https://doi.org/10.1061/\(asce\)st.1943-541x.0001820](https://doi.org/10.1061/(asce)st.1943-541x.0001820)
- Arabzadeh, H., & Galal, K. (2018). Seismic-Response Analysis of RC C-Shaped Core Walls Subjected to Combined Flexure, Shear, and Torsion. *Journal of Structural Engineering*, 144(10), 04018165. [https://doi.org/10.1061/\(asce\)st.1943-541x.0002181](https://doi.org/10.1061/(asce)st.1943-541x.0002181)
- ASCE/SEI 41-17. (2017). *Seismic Evaluation and Retrofit of Existing Buildings* (ASCE/SEI 4). American Society of Civil Engineers. <https://doi.org/10.1061/9780784414859>
- ASCE. (2014). *Seismic evaluation and retrofit of existing buildings*.
- ASCE7-16 Minimum Design Loads and Associated Criteria for Buildings and Other Structures. (2016). *ASCE7-16 Minimum Design Loads and Associated Criteria for Buildings and Other Structures*.
- ATC. (2009). Quantification of building seismic performance factors. *Fema P695, June*, 421.
- Azam, S. K. M., & Hosur, V. (2013). Seismic Performance Evaluation of Multistoried RC framed buildings with Shear wall. *International Journal of Scientific & Engineering Research*, 4(1), 1.
- Constantin, R. (2016). *Seismic behaviour and analysis of U-shaped RC walls*. 7133.
- El-Tawil, S., Fortney, P., Harries, K., Shahrooz, B., Kurama, Y., Hassan, M., & Tong, X. (2009). Recommendations for seismic design of hybrid coupled wall systems. In *Recommendations for Seismic Design of Hybrid Coupled Wall Systems*. <https://doi.org/10.1061/9780784410608>
- Harries, K. A. (2001). Ductility and deformability of coupling beams in reinforced concrete coupled walls. In *Earthquake Spectra* (Vol. 17, Issue 3, pp. 457–478). <https://doi.org/10.1193/1.1586184>
- Huret, R. (2017). 5. Federal Emergency Management Agency. *Katrina, 2005, November*, 163–189. <https://doi.org/10.4000/books.editionsehess.939>
- Khalid Mosalam, Amarnath Kasalanati, Grace Kang, C. B.-A. (2011). *Pacific Earthquake Engineering Research Center*.
- Lu, X., Tian, Y., Cen, S., Guan, H., Xie, L., & Wang, L. (2018). A high-performance quadrilateral flat shell element for seismic collapse simulation of tall buildings and its implementation in OpenSees. *Journal of Earthquake Engineering*, 22(9), 1662–1682.
- Lu, X., Xie, L., Guan, H., Huang, Y., & Lu, X. (2015). A shear wall element for nonlinear seismic analysis of super-tall buildings using OpenSees. *Finite Elements in Analysis and Design*, 98, 14–25. <https://doi.org/10.1016/j.finel.2015.01.006>

- McKenna, F. (2011). OpenSees: a framework for earthquake engineering simulation. *Computing in Science & Engineering*, 13(4), 58–66.
- Moehle, J., Bozorgnia, Y., Jayaram, N., Jones, P., Rahnama, M., & Shome, N. (2011). Case Studies of the Seismic Performance of Tall Buildings Designed by Alternative Means – Task 12 Report for the Tall Buildings Initiative: Final Report to California Seismic Safety Commission and California Emergency Management Agency. *Pacific Earthquake Engineering Research Center*, July.
- Ren, P., Li, Y., Guan, H., & Lu, X. (2015). Progressive Collapse Resistance of Two Typical High-Rise RC Frame Shear Wall Structures. *Journal of Performance of Constructed Facilities*, 29(3), 04014087. [https://doi.org/10.1061/\(asce\)cf.1943-5509.0000593](https://doi.org/10.1061/(asce)cf.1943-5509.0000593)
- Saleemuddin, M., Mohd, Z., & Sangle, K. K. (2017). Seismic damage assessment of reinforced concrete structure using non-linear static analyses. *KSCE Journal of Civil Engineering*, 21(4), 1319–1330.
- Wu, Y., Wang, B., Yang, Y., & Fu, J. (2019). Nonlinear Optimization for Geometric Parameters of Reinforced Concrete Coupled Structural Walls. *KSCE Journal of Civil Engineering*, 23(10), 4339–4353. <https://doi.org/10.1007/s12205-019-1189-5>
- Zaker Esteghamati, M., Banazadeh, M., & Huang, Q. (2018). The effect of design drift limit on the seismic performance of RC dual high-rise buildings. *The Structural Design of Tall and Special Buildings*, 27(8), e1464.
- Zhang, P., Restrepo, J. I., Conte, J. P., & Ou, J. (2017). Nonlinear finite element modeling and response analysis of the collapsed Alto Rio building in the 2010 Chile Maule earthquake. *Structural Design of Tall and Special Buildings*, 26(16). <https://doi.org/10.1002/tal.1364>